

Determination of Cloud Base Height Using the GSFC Raman Lidar

*B. B. Demoz, K. D. Evans, M. Cadirola, and S. H. Melfi
University of Maryland, Baltimore County
Baltimore, Maryland*

*D. O’C. Starr, D. N. Whiteman, and G. Schwemmer
National Aeronautics and Space Administration
Goddard Space Flight Center
Greenbelt, Maryland*

*D. L. Hlavka and J. R. Campbell
Science Systems and Applications, Inc.
Greenbelt, Maryland*

*D. D. Turner
Pacific Northwest National Laboratory
Richland, Washington*

Introduction

Exact determination of cloud geometry is important in climate and radiation studies. The derivation of cloud optical depth, for example, requires accurate determination of cloud base height (CBH) and top height. Recent studies by Kogan and Kogan (1998) suggest that variations in cloud boundary (base and top heights) may be more important than variations in cloud microstructure for the calculation of cloud optical depth. They report that neglect of irregular cloud boundary (slab assumption) could lead to 20% to 45% errors in optical depth calculations. Further, Pincus et al. (1999) report that cloud top is “uncorrelated with optical thickness,” suggesting that CBH and/or cloud droplet concentration may be the primary controlling factor. Moreover, Han and Ellingson (1997) indicate that the major uncertainty in the calculation of downwelling longwave flux at the surface may be due to errors in determining cloud thickness. Thus, an accurate characterization of CBH is required.

This study reports on determination of CBH using the Goddard Space Flight Center (GSFC) Scanning Raman Lidar (SRL). We focus on the advantages the SRL introduces in the determination of CBH in comparison to determinations made using data from the Micropulse Lidar (MPL), Belfort Laser Ceilometer (BLC), and Millimeter-Wavelength Cloud Radar (MMCR). The SRL observations provide quantitative Aerosol Scattering Ratio (ASR), water vapor mixing ratio (W), and relative humidity (RH, derived quantity) profiles not available from the other sensors. Data from the U.S. Department of Energy (DOE) Atmospheric Radiation Measurement (ARM) Program’s Cloud and Radiation Testbed (CART) site and other experiment campaigns are utilized.

Derivation of CBH

In general, CBH can easily be detected from the lidar return signal as the altitude where the signal reaches its highest value (Eberhard 1986). Thus, most techniques search for “true” zero crossings in the derivative of the returned signal (Pal et al. 1992; Campbell et al. 1998; Gaumet et al. 1995). The estimated extinction profile is often used to minimize the effect of the lower atmosphere on the ASR.

Although CBH is routinely assumed to be the location of the peak in the lidar backscatter signal, it is well known that this may be an overestimation; the difference in altitude between the point where the signal starts to increase and its peak can be as large as 800m (Pal et al. 1992). Problems also arise when the lidar signal does not undergo a sudden change (as in fog or the initial phase of cloud formation), when multiple peaks occur in the signal (multiple cloud layers), and at times of precipitation or haze between cloud and the instrument. Rain and virga introduce large errors in the detection of “true” CBH. The addition of an extra signal, the water vapor channel, provides data that may be used to resolve some of these problems. The vapor profile can be used directly or converted to RH, using sonde temperature profiles.

Examples

Warm Cloud Case

Figure 1 shows analysis of SRL, BLC, MPL, and sonde data for September 28, 1997, over the DOE ARM CART site near Lamont, Oklahoma. Microwave Radiometer (MWR) liquid water data are also included as “cloud” indicators. Rigorous analysis of SLR and other data sets indicated that the clouds were formed as a result of convergence lifting of low level moist air followed by mixing with cold and dry air at higher levels. A number of points can be made here concerning CBH:

Aerosol Channel: While the BLC (black), SRL (red triangles), and MPL (green) all tracked each other well, the BLC estimates were consistently higher. The SRL and BLC also did not detect any cloud at 1-km height between 0500 Universal Time Coordinates (UTC) and 0600 UTC as the MPL indicates. But, despite the use of a simple definition for cloud onset (ASR value of 2.5 times the background), the SRL-derived CBH agreed very well with that of the MPL. The MPL routine for CBH essentially searches for zero crossings in the derivative of the lidar signal. A comparison of the dew point depression (T-Td) profile derived from the sonde with the aerosol channel profile shows that the location of the peak aerosol return overestimates CBH (taken to be where T-Td = 0) by about 100 m, while a simple use of 2.5 for ASR does well for this specific case. Note that the “fog” layer before 0530 UTC detected by the SRL (blue circles), and not reported by MPL and BLC, had ASR values of about twice the background value. Further, the MPL and BLC report of multiple cloud layers between the altitudes of 2.5 km and 4.0 km around 0600 UTC may be a result of complications due to virga, as indicated by the MMCR (not shown here).

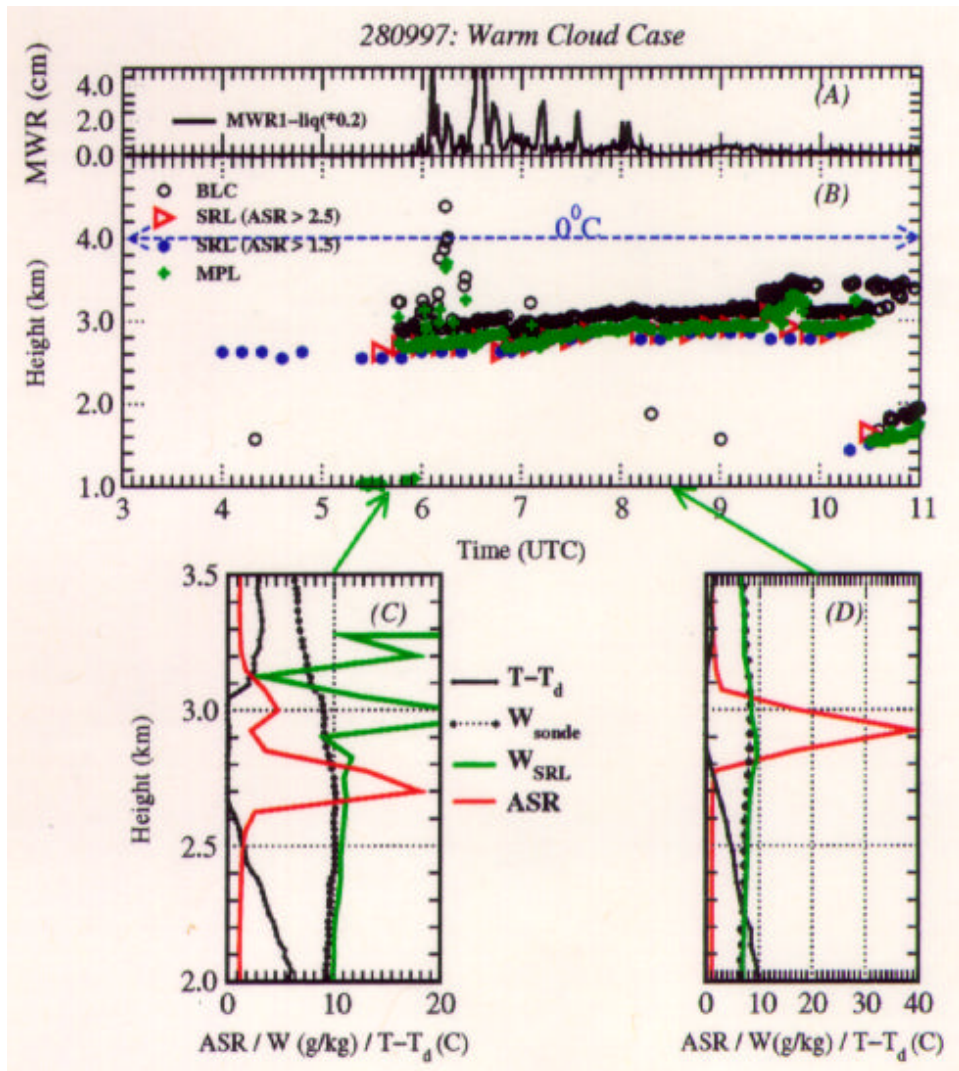


Figure 1. Time series of MWR liquid water (a), and SRL (blue and red), BLC (black), MPL (green) derived CBH (b). Profiles of SRL measured ASR (red) and W (blue) are also compared to sonde derived dewpoint depression ($T-T_d$, black) and W (black) at 0530 UTC (d) and 0830 UTC (e). Panel (c) gives an example of “background” ASR values at 0200 UTC (solid curve) and 0430 UTC (dashed).

Water Vapor Channel: SRL water vapor profiles show the moistening of the layer leading to cloud formation and thus offer a better understanding and definition for the onset of cloud (thus, CBH even in conditions of virga and precipitation) while at the same time elucidating the dynamics of the atmosphere leading to the cloud formation. The SRL-derived RH profile at 0530 UTC indicated saturation at about 100 m lower than the sonde, mainly due to higher mixing ratio values at these altitudes. This excessive moisture is believed to be caused by detection of Raman signal from rain drops, also observed at the time by the MMCR. Virga, and its effect on CBH estimation, are easily corrected by choosing narrow filters in the SRL (Whiteman et al. 1999). However, it may also be used as a direct CBH indicator, for it adds very little error to the observed mixing ratio. By 0830 UTC, precipitation stopped (confirmed by

MMCR) and thus no “vapor excess” due to virga was observed. For single-channel aerosol instruments, the detection of virga is problematic and may lead to errors in cloud boundary estimation, as we suspect may be the case in the MPL- and BLC-indicated multiple cloud layers around 0600 UTC (see next section for more on this).

Mixed Phase Case

Recent improvements in the SRL allowed the instrument to be operated during precipitating conditions. An example of data during such conditions, observed at Andros Island, Bahamas, is shown in Figure 2. ASR (black) and vapor (green) profiles are shown at three selected times: at 0400 UTC when precipitation reached the ground, at 0745 UTC and coincident with a rawinsonde, and at 1020 UTC

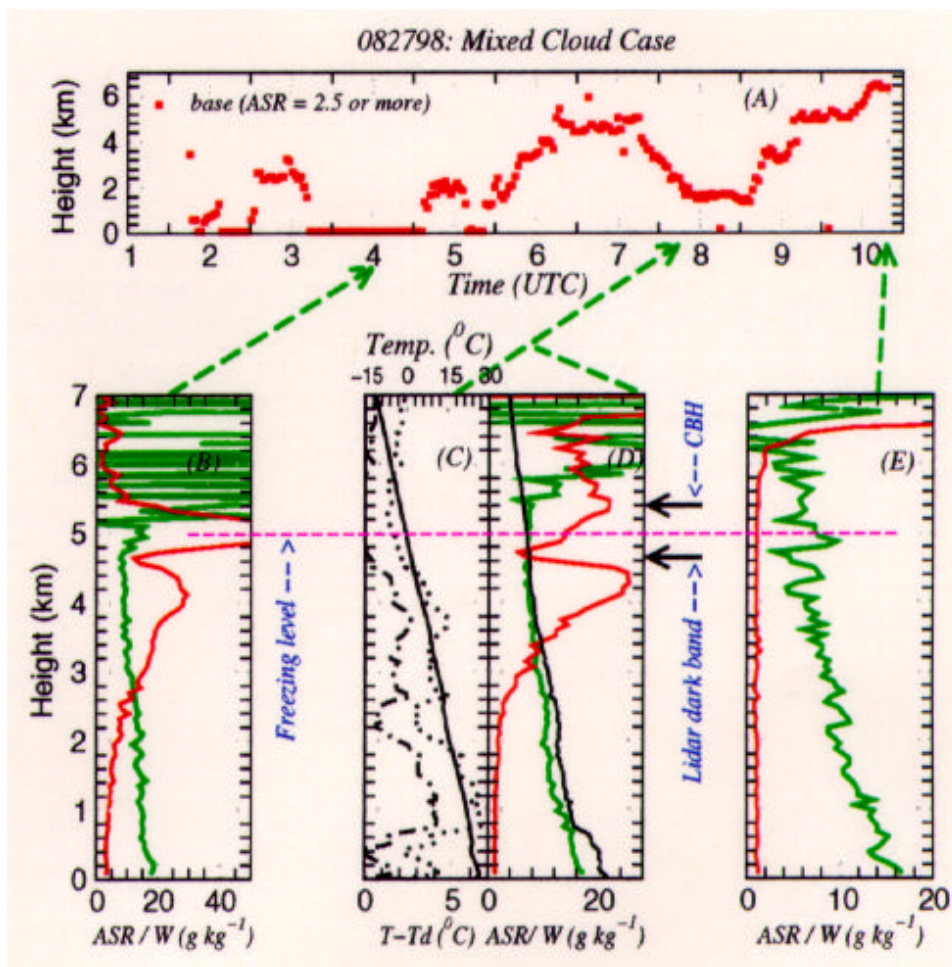


Figure 2. Time series of CBH (a), ASR (black) and W (green) profiles at three selected times: 0400 UTC (b), 0745 UTC (d) and 1020 UTC (e) and sonde profiles (c) of temperature (red) and both the “corrected” and uncorrected (dotted) dewpoint depression (violet) profiles are shown. The sonde derived mixing ratio (black) is also shown in (c) for comparison.

when precipitation stopped. The CBH time series (defined as ASR of 2.5 or greater) during the 10 hours of operation is also shown. At 0400 UTC, the ASR near the surface was about five times greater than the background with a local minimum at about 4.6 km, before it peaked again. Using only this information, it would be difficult to get a correct CBH (zero crossing of the ASR derivative). However, the SRL vapor channel may be used to resolve this problem. The point where the vapor signal gets highly attenuated indicates cloud and thus CBH, which was at about 5 km. At 0745 UTC, the aerosol profile had a similar shape to that at 0400 UTC but with close to background values at the lowest levels, an indication that precipitation no longer reached the ground. Again, the vapor mixing ratio profile indicates cloud at 5.4 km, which coincides with a peak in the ASR and the level of the lowest value of uncorrected dewpoint depression (black, dotted). (Note: the sonde-derived dewpoint measurements had documented problems during this time and are in the process of being corrected by the manufacturer.) By 1020 UTC, precipitation had stopped and CBH was at 6.4 km, an ideal ASR profile. Note that the persistent minima at about 700 m below the CBH and about 300 m below the freezing level is the “lidar dark band” (Sassen and Chen 1995), which is believed to be due to the structural collapse of melted snowflakes and their transition to spherical drops.

Cold Cloud Case

SRL and sonde data are shown in Figure 3 for a cold cloud case observed on November 25, 1991, at Coffeyville, Kansas. The SRL revealed a progressively lowering CBH (defined using $ASR = 2.5$ again). Profiles of SRL data at 0200 UTC and 0500 UTC are also compared with rawinsonde RH profiles revealing that the saturation ($RH(\text{water}) = 95\%$ and $RH(\text{ice}) > 100\%$) occurred at about ASR of two and half times background. Peak values in the aerosol signal occurred 300 m to 500 m or more above the saturation point. For both profiles, the mixing ratio increases slightly above cloud base, possibly indicating a layer dominated by evaporating precipitation particles, hence the continued lowering of CBH. The steady decrease in the altitude of the top and the eventual moistening of the dry layer between 2.5 km and 3.5 km before 0230 UTC in Figure 4 is supporting evidence for this speculation.

Conclusion

We have illustrated possible problems in present methods used to determine CBH from measurements with single aerosol channel lidar instruments. In some cases, the errors can be substantial. An alternative approach based on application of SRL-derived aerosol scattering ratio and water vapor mixing ratio profile information yields a less ambiguous determination. In particular, it is possible to distinguish precipitation and virga from the “true” cloud base. Fog is also detected. Thus, SRL offers significant advantages even for CBH determination.

We have discussed the possibility that present derivation of CBH using single aerosol channel instruments may lead to substantial error. These are mainly due to the ambiguous definition of “cloud base” and/or lack of resolving precipitation or virga. We have demonstrated here ways of using the additional information that is derived from the SRL water vapor profile to resolve these problematic issues. With the planned improvements in vertical and temporal resolution, the SRL has great potential towards resolving and even defining cloud boundary determination parameters.

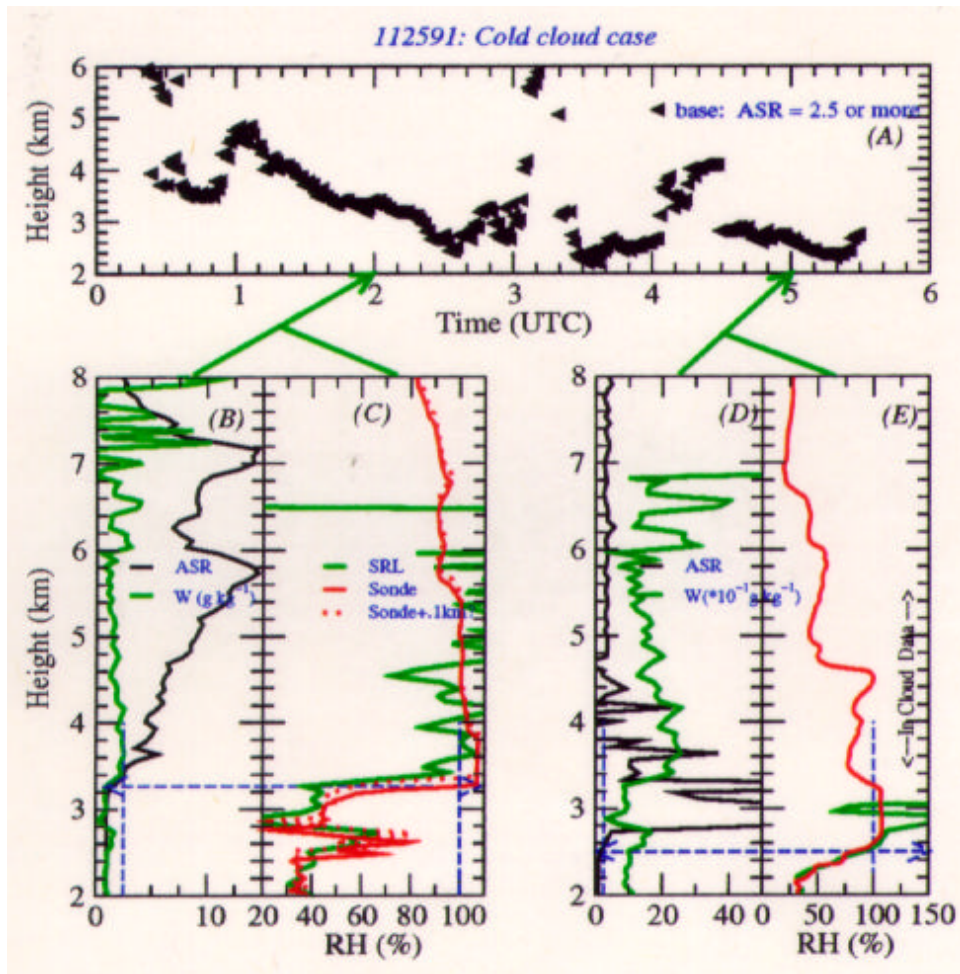


Figure 3. Time series of SRL-derived CBH (a), and profiles of SRL data at 0200 UTC (b) and 0500 UTC (d) showing ASR (black) and water vapor (green). Sonda (red) and SRL (black) measured profiles of RH (red) and at 0200 UTC (c) and 0500 UTC (e) are also compared.

Acknowledgments

This research was supported by the U.S. Department of Energy's Environmental Science Division as part of the ARM Program.

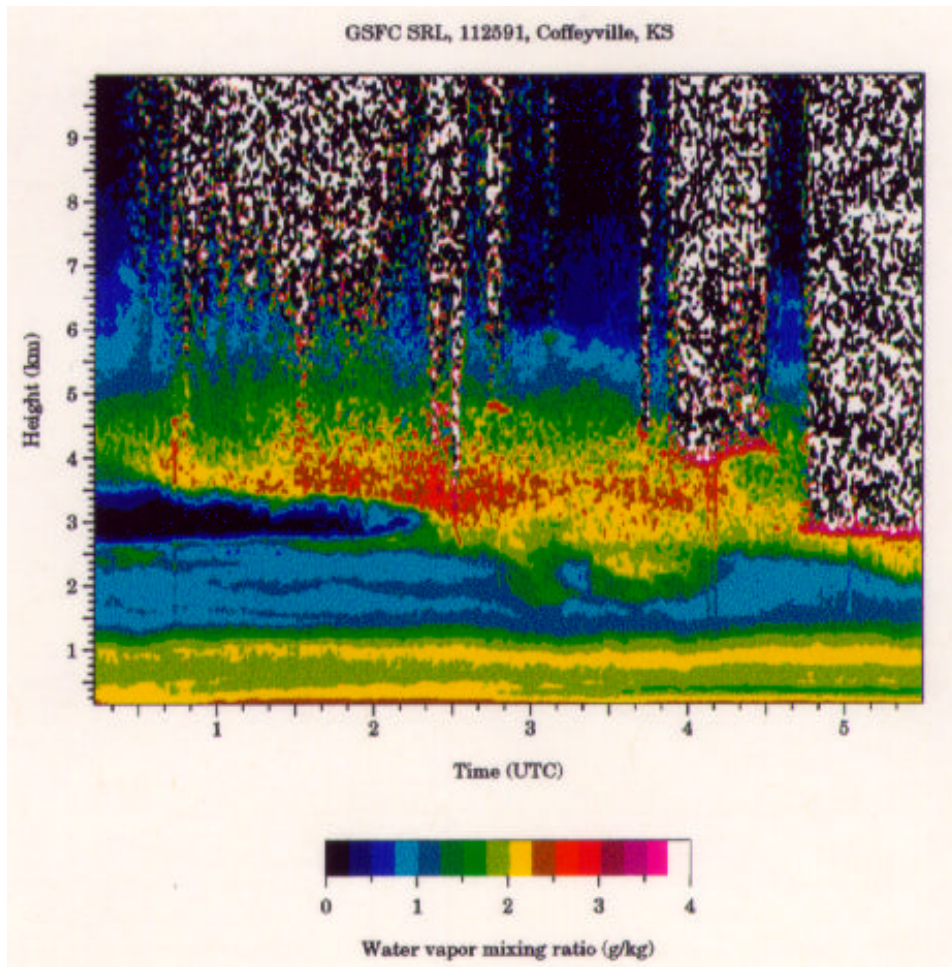


Figure 4. SRL-sensed water vapor mixing ratio (g kg^{-1}) profiles on November 25, 1991, over Coffeyville, Kansas. Note the vertical stipling, which indicates attenuation by cloud.

References

Campbell, J. R., D. L. Hlavka, J. D. Spinhirne, D. D. Turner, and C. J. Flynn, 1998: Operational cloud boundary detection and analysis from micro pulse lidar data. In *Proceedings of the Eighth Atmospheric Radiation Measurement (ARM) Science Team Meeting*, DOE/ER-0738, pp. 119-122. U.S. Department of Energy, Washington, D.C.

Eberhard, W. L., 1986: Cloud signals from lidar and rotating beam ceilometer compared with pilot ceiling. *J. Atmos. Oceanic Technol.*, **3**, 499-512.

Gaumet, J. L., J. C. Heinrich, O. Peyrat, M. Cluzeau, P. Pierrard, and J. Prieur, 1995: Cloud base height measurements with a single pulse Erbium glass laser ceilometer. In *Proceedings of the 9th Symposium on Meteorological Observation and Instrumentation*, pp. 101-105. American Meteorological Society.

Han, D., and R. G. Ellingson, 1997: A test of the validity of cumulus cloud parameterizations for longwave radiation calculations. In *Proceedings of the Seventh Atmospheric Radiation Measurement (ARM) Science Team Meeting*, CONF-970365, pp. 27-31. U.S. Department of Energy, Washington, D.C.

Kogan, Z. N., and Y. L. Kogan, 1998: The effect of cloud geometrical thickness variability on optical depth. In *Proceedings of the Eighth Atmospheric Radiation Measurement (ARM) Science Team Meeting*, DOE/ER-0738, pp. 377-380. U.S. Department of Energy, Washington, D.C.

Pal, S. R., W. Steinbrecht, and A. Carswell, 1992: Automated method for lidar determination of cloud-base height and vertical extent. *Applied Optics*, **31**, 1488-1494.

Pincus, R., A. Marshak, M. Gunshore, and W. Wiscombe, 1999: The topography of cloud tops. This Proceedings.

Sassen, K., and T. Chen, 1995: The lidar dark band: An oddity of the radar bright band analogy. *Geophys. Res. Lett.*, **22**, 3505-3508.

Whiteman, D. N., and S. H. Melfi, 1999: Cloud liquid water detection using Raman scattering. This Proceedings.